International Journal of Future Generation Communication and Networking
Vol. 9, No. 3 (2016), pp. 123-138
http://dx.doi.org/10.14257/ijfgcn.2016.9.3.12

A Novel TOA Estimation Algorithm Based on Kurtosis and Standard Slope in the 60GHz Sensor Network

Xiao-Lin Liang[1], Hao Zhang[1, 2], Ting-Ting Lu[1], T. Aaron. Gulliver[2] and Xue-rong Cui[3]

[1]*College of Information Science and Engineering, Ocean University of China, Qingdao, 266100, China;*
[2]*Department of Electrical and Computer Engineering, University of Victoria, Victoria V8W 3P6, Canada*
[3]*Department of Computer and Communication Engineering, China University of Petroleum (East China),*
xiaolin87liang@163.com, zhanghao@ouc.edu.cn,
lvtingting33@163.com, agullive@ece.uvic.ca
cuixuerong@163.com

Abstract

Accurate localization has gained significant interest in the field of sensor networks, but Time of Arrival (TOA) estimation algorithms which based coherent by Matched Filter are not practical for low cost, low complexity impulse-radio 60GHz ranging, localization and tracking systems because of the high sampling rate. In this paper, a novel TOA estimation algorithm which based on non-coherent by Energy Detection is presented where TOA is estimated via Threshold Crossing. The expected values of Standard Slope, Maximum Slope, Kurtosis and Standard Deviation with respect to the Signal to Noise Ratio (SNR) are investigated using the IEEE 802.15.3c Channel Models. It is shown that the Kurtosis and Standard Slope are more sensitive to the SNR and thus they are even much more suitable for TOA estimation. In order to improve the precision of TOA estimation based on Energy Detection, a novel TOA estimation algorithm which is based on a joint metric of the Standard Slope and Kurtosis is proposed. The best threshold values for different SNRs are investigated and the effects of integration period and channel models are examined. In comparison with other algorithms which based on Energy Detection, the results show that in both the CM1.1 and CM2.1 channels, the joint metric provides higher precision and robustness.

Keywords: 60GHz, TOA estimation, ranging, Kurtosis, Standard Slope

1. Introduction

The demand for high data rate wireless communications with low latency has increased dramatically in recent years. Unfortunately, due to spectrum limitations and transmit power regulations, current short-range wireless communication strategies cannot achieve Gigabit per second (Gbps) data rates. Fortunately, wireless communications in the 60GHz millimeter wave (mm-wave) band has become viable for Gbps wireless communication networks [1-4] due to the availability of several GHz of license-free spectrum, up to 10W maximum transmit power, no interference from other systems, and the development of low-cost Complementary Metal-Oxide Semiconductor (CMOS) devices. The Federal Communications Commission (FCC) permits communications in the 60GHz unlicensed band at an Effective Isotropic Radiated Power (EIRP) of up to 40dBm, which is many times greater than other short-range wireless communication strategies. In China, this limit is 44dBm [5]. Although the Path Loss (PL) is high at 60GHz, the received power

ISSN: 2233-7857 IJFGCN

can still be significant. Impulse radio communication strategies have been proposed for this frequency band because it can be effective in separating the multipath signals at the receiver. This is because short pulses are employed for communications with a duration (typically under 100 picoseconds), which is far less than the multipath propagation delay. These signals can also provide the fine multipath resolution required for high precision ranging and localization [6]. Thus, 60GHz signals are even much suitable for localization applications for short distances.

Generally, the localization strategies can be classified into range based [7-10] and non-range based [11]. For example, TOA [10, 12] and Time Difference of Arrival (TDOA) [10] are range based strategies, while Received Signal Strength (RSS) and Angle of Arrival (AOA) [11] are non-range based. Localization that based on range (TOA or TDOA) is even much suitable for using with IR-60GHz strategy [11], as it can take full advantage of the higher time and multipath resolution available with very short IR-60GHz signals. TOA estimation which is even much more accurate is the key to accurate ranging, but this is very challenging due to the potentially hundreds of multipath components in 60GHz channels, even in the Non-line of Sight (NLOS) environments.

TOA estimation has been extensively studied [12, 15-18] for the past few years. There are two approaches which are much more applicable for TOA estimation, a Matched Filter (MF) [16] (such as a RAKE or correlation receiver) with a higher sampling rate and higher precision correlation, or an Energy Detector [18] with a lower sampling rate and lower complex. A MF is the optimal strategy for TOA estimation, where a correlator template is matched exactly to the received signal. However, a receiver operating at the Nyquist sampling rate makes it very difficult to align with the multipath components of the received signal [15]. In addition, a MF requires a priori estimation of the channel, including the timing, fading coefficient, and pulse shape for each component of the impulse response [15]. Because of the higher sampling rates and channel estimation, a MF may not be practical in many applications. As opposed to a more complex MF, an Energy Detection is a non-coherent approach to TOA estimation. It consists of a square-law device, followed by an integrator, sampler and a decision mechanism. The TOA estimate is made by comparing the integrator output with a threshold and choosing the first sample to exceed the threshold. This is a convenient strategy that directly yields an estimate of the start of the received signal. Thus, a low complexity, low sampling rate receiver can be employed without the need for a priori channel estimation.

The major challenge with Energy Detection is the selection of an appropriate threshold based on the received signal samples. In [17], a normalized threshold selection strategy for TOA estimation was proposed which exploits the kurtosis of the received samples. In [18], an approach based on the minimum and maximum sample energy was introduced. Threshold selection for different SNR values was investigated via simulation. These approaches have limited TOA precision, as the strongest path is not necessarily the first arriving path.

In this paper, we consider the relationship between the SNR and the statistics of the integrator output including Standard Slope, Maximum Slope, Kurtosis and Standard Deviation. A metric based on Kurtosis and Standard Slope is then developed for threshold selection. The threshold for different SNR values is investigated and the effects of the integration period and channel are examined. Performance results are presented which show that in both the CM1.1 and CM2.1 channels, this joint metric provides higher precision and robustness. The remainder of this paper is organized as follows. In Section 2 the system model is outlined. Section 3 discusses various TOA estimation algorithms based on Energy Detection. Section 4 considers the statistical characteristics of the energy values. In Section 5 a joint metric based on K and SS is proposed, and a novel TOA estimation algorithm is introduced. Section 6 presents some performance results, and Section 7 concludes the paper.

2. System Model

Currently, there are two important standards that have been developed for 60GHz wireless communications systems, IEEE 802.15.3c and IEEE 802.11ad [19-20]. In this paper, the channel models in IEEE 802.15. 3c standard are used because it is specifically designed for Wireless Personal Area Networks (WPAN) and thus encompasses typical indoor environments. Further, these are the most widely employed models for 60GHz systems. The IEEE 802.15.3c standard was the first developed for high data rate short-range wireless systems. The physical layer was designed to support the transmission of data within a few meters at a minimum data rate of 2Gbps. These models have been developed for communications in the frequency band 57 to 66GHz in indoor residential, indoor office and library environments (with differences largely due to the LOS and NLOS characteristics) [21-25].

In this paper, a Pulse Position Modulation Time Hopping (PPM-TH) 60GHz signal is employed for ranging purposes. The propagation delay $\hat{\tau}$, between the transmitter and receiver is estimated for use in localization.

2.1. 60GHz Signal

The PPM-TH 60GHz signals have a very short duration (typically 100 picoseconds or less), and can be expressed as

$$s(t)=\sum_{-\infty}^{\infty} p\left(t-jT_s-C_jT_c-a_j\varepsilon\right) \tag{1}$$

Where T_s is the symbol time. The Time Hopping (TH) code represented by C is a pseudorandom integer-valued sequence which is unique for each user to limit multiple access interference, and T_c is the chip time. The PPM time shift is ε so that if a_j is 1, the signal is shifted in time by ε, while if a_j is 0, there is no shift. Many pulse shapes have been proposed for 60 GHz systems. In this paper a Gaussian pulse is employed which is multiplied by the carrier signal to give [26]

$$p(t)=\frac{\sqrt{2}}{\alpha}\exp\left(-2\pi\frac{t^2}{\alpha^2}\right)\cos\left(2\pi f_c t\right) \tag{2}$$

Where α is the shape factor, and f_c is the carrier frequency which here is $f_c=60$ GHz. A smaller shape factor results in a shorter duration pulse and a larger bandwidth.

2.2. Multipath Fading Channel

The received signal can be written as

$$r(t)=\sum_{n=1}^{N}\alpha_n p\left(t-\tau_n\right)+n(t) \tag{3}$$

Where N is the number of received multipath components, α_n and τ_n denote the amplitude and delay of the nth path respectively, $p(t)$ is the received 60GHz pulse and $n(t)$ is Additive White Gaussian Noise (AWGN) with zero mean and two sided power spectral density $N_0/2$. Equation (3) can be rewritten as

$$r(t)=s(t)*h(t)+n(t) \tag{4}$$

Where $s(t)$ is the transmitted signal, and $h(t)$ is the channel impulse response which

can be expressed as

$$h(t,\theta)=\sum_{k=1}^{K}\sum_{l=1}^{L_k}\mu_{kl}\delta\left(t-T_k-\tau_{kl}\right)\delta\left(\theta-\theta_k-\omega_{kl}\right) \quad (5)$$

Where $\delta(.)$ is the dirac-delta function, K is the number of clusters, L_k is the number of rays in the k^{th} cluster, and μ_{kl}, τ_{kl} and ω_{kl} denote the complex amplitude, delay and azimuth of the k^{th} ray of the l^{th} cluster, respectively. Similarly, T_k and θ_k represent the delay and mean Angle of Arrival (AOA) of the k^{th} cluster.

2.3. Energy Detection

As shown in Figure 1 [27], after the amplifier, the received signals are squared, and then input to an integrator with integration period T_i. Because of the inter-frame leakage due to multipath signals, the integration duration is $3T_f/2$, so the number of signal values for Energy Detector is N= $3T_f/2T_i$. The integrator outputs can be expressed as:

$$z[n]=\sum_{i=1}^{N}\int_{(i-1)T_f+(c_j+n)Ti}^{(i-1)T_f+(c_j+n-1)Ti} r^2(t)dt \quad (6)$$

Where $n\in\{1,2,..,N\}$ denotes the sample index with respect to the starting point of the integration period and N is the number of pulses per symbol. Here, N is set to 1, so the integrator outputs are

$$z[n]=\sum_{i=1}^{N}\int_{(c_j+n-1)T_i}^{(c_j+n)T_i} r^2(t)dt \quad (7)$$

The final output of integrator is shown in the Figure 2.

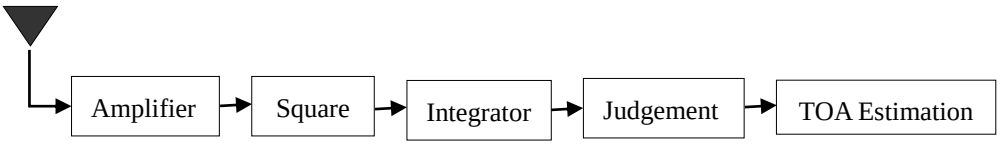

Figure 1. Block Diagram of the Energy Detector Receiver

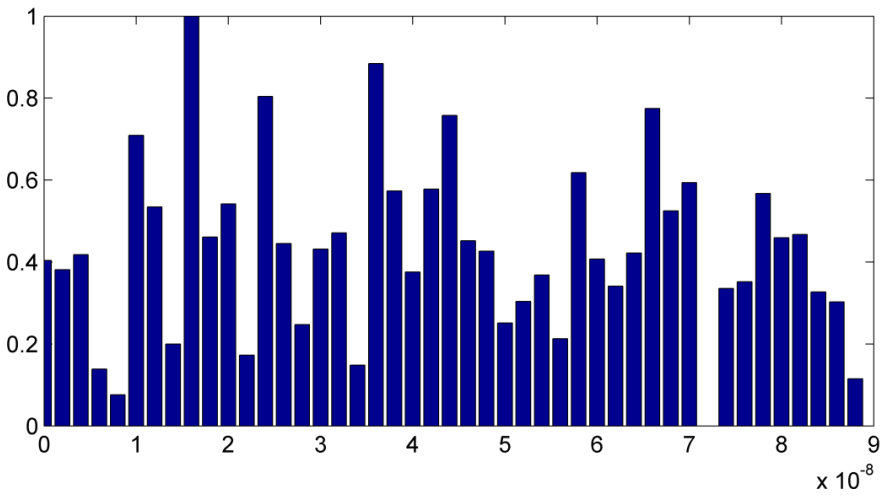

Figure 2. Output of the Energy Detector Receiver

If $z[n]$ is the integration of noise only, it has a centralized Chi-square distribution, while it has a non-centralized Chi-square distribution if a signal is present. The mean and variance of the noise and signal values are given by [17] respectively.

$$\mu_0 = F\sigma^2, \sigma_0 = 2F\sigma^4 \quad (8)$$

$$\mu_e = F\sigma^2 + E_n, \sigma_e^2 = 2F\sigma^4 + 4\sigma^2 E_n \quad (9)$$

Where E_n, is the signal energy within the nth integration period and F is the number of degrees of freedom given by $F = 2BT_i + 1$. Here B is the signal bandwidth.

3. TOA Estimation Based on Energy Detection

3.1. TOA Estimation Algorithms

There are many TOA estimation algorithms based on Energy Detection for determining the start block of a received signal, as show in Figure 2. The simplest is Maximum Energy Selection (MES), which chooses the maximum energy value to be the start of the signal value. The TOA is estimated as the center of the corresponding integration period

$$\tau_{MES} = \left[\arg\max_{1 \le n \le N_b} \{ z[n] \} - 0.5 \right] T_i \quad (10)$$

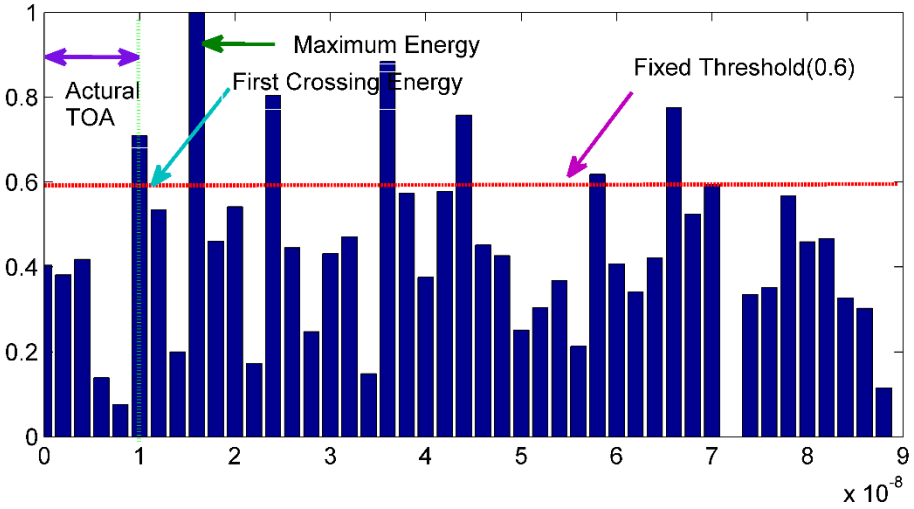

Figure 3. TOA Estimation Based on Energy Detection

However, as show in Figure 3, the maximum energy value may not be the first energy block [13], especially in NLOS environments. On average, the first energy value $z[n]$ is located before the maximum $z[n_{\max}]$, i.e. $n \le n_{\max}$. Thus, TC TOA estimation has been proposed where the received energy values are compared to an appropriate threshold ξ. In this case, the TOA estimation is given by

$$\tau_{TC} = \left[\arg\min_{1 \le n \le n_{\max}} \{ n \mid z[n] \ge \xi \} - 0.5 \right] T_i \quad (11)$$

It is difficult to determine an appropriate threshold ξ directly, so usually a normalized threshold ξ_{norm} is calculated. Using ξ_{norm}, ξ is given by

$$\xi = \xi_{norm}\left(\max\left(z(n)\right) - \min\left(z(n)\right)\right) + \min\left(z(n)\right) \quad (12)$$

The TOA (τ_{TC}) is then obtained using (11). A simpler TC algorithm is the Fixed Threshold (FT) algorithm where the threshold is set to a fixed value, for example ξ_{norm} =0.4 .The problem in this case becomes one of how to set the threshold. It should be based on the statistics of the signal energy, particularly for multipath, NLOS indoor environments.

3.2. Error Analysis

The Mean Absolute Error (MAE) of TOA estimation based on TC was analyzed, and closed form error expressions derived. The MAE can be used to evaluate the quality of an algorithm, and is defined as

$$MAE = \frac{1}{N}\sum_{n=1}^{N}\left(t_n - t_n\right) \quad (13)$$

Where t_n is the nth actual propagation time, t_n is the nth TOA estimate, and *N* is the number of TOA estimates.

4. Statistical Characteristics

Maximum Slope, Kurtosis, Standard Slope and Standard Deviation of the energy blocks are analyzed in this section.

4.1. Kurtosis

The Kurtosis is calculated using the second and fourth order moments and is given by

$$k = \frac{E\left[\left(x_i - \mu_x\right)^4\right]}{E\left[\left(x_i - \mu_x\right)^2\right]^2} = \frac{E\left[\left(x_i - \mu_x\right)^4\right]}{\sigma_x^4} \quad (14)$$

Where μ_x is the mean value and σ_x is the Standard Deviation. The Kurtosis for a standard normal distribution is three. For this reason, Kurtosis is often redefined as $K = K - 3$(often referred to as "excess *K*"), so that the standard normal distribution has a *K* of zero, positive *K* indicates a "peaked" distribution and negative *K* indicates a "flat" distribution. For noise only (or for a low SNR) and sufficiently large *F* (degrees of freedom of the Chi-square distribution), $z[n]$ has a Gaussian distribution and *K*=0. On the other hand, as the SNR increases, *K* will tend to increase.

4.2. Maximum Slope

Kurtosis cannot account for delay or propagation time, so the slope of the energy values is considered as a measure. These values are divided into (N-M+1) groups, with M values in each group. The slope for each group is calculated using a least squares line-fit. The Maximum Slope can then be expressed as

$$MS = \max_{1 \le n \le N-M+1} slope\left\{linefit\left(z[n], z[n+1], ..., z[n+M-1]\right)\right\} \quad (15)$$

4.3. Standard Deviation

The Standard Deviation is a widely used measure of variability. It shows how much

variation or "dispersion" there is from the average (mean or expected value). The Standard Deviation is given by

$$D = \sqrt{\frac{\sum_{i=1}^{N}\left(x_i - \mu_x\right)^2}{N-1}} \tag{16}$$

4.4. Standard Slope

In order to account for both gradient and the dispersion at the same time, we design a parameter Standard Slope which can be expressed as

$$S_s = \max\sqrt{\frac{\sum_{i=1}^{N}\left(x_i - \mu_x\right)^2}{N-1}\left[meank\left(x_i, T_i, \mathrm{g}\right)\right]^2} \tag{17}$$

Where the T_i is the integration period, g is the number of energy block which are used to calculate the gradient of the energy.

4.5. Characteristics of the Four Parameters

In order to examine the characteristics of the four parameters (Maximum Slope, Kurtosis, Standard Slope and Standard Deviation), the CM1.1 (residential LOS) and CM2.1 (residential NLOS) channel models from the IEEE802.15.3c standard are employed. For each SNR value, 1000 channel realizations are generated and sampled at $f_c = 1 \cdot e^{10}$ Hz. The other system parameters are $T_f = 200ns$, $T_c = 1ns$, the value of T_i is from 1ns to 4ns and N=1. Each realization has a TOA uniformly distributed within (0 - T_f).

The four parameters were calculated, and the results obtained are shown in from Figures 4-7. This results show that the characteristics of the parameters with respect to the SNR are similar for the two channels. Further, from Figures 4-7, we can see that the Kurtosis increases as the SNR increases both in channel CM1.1 and CM2.1. Conversely, the Standard Slope and Standard Deviation decrease with the increase of the SNR, but the Standard Slope changes more rapidly in comparison with other parameters. At the same time, Maximum Slope decrease with the increase of the SNR when SNR<16dB, but increase with the increase of the SNR when SNR>16dB, so it can't reflect the SNR information better. Since the Standard Slope change more rapidly than Standard Deviation, it better reflect changes in SNR, and so it is more suitable for TOA estimation. Moreover, when the SNR is less than 17dB, Kurtosis changes slowly while the Standard Slope changes rapidly. On the other hand, when the SNR is higher than 17dB, the Kurtosis changes rapidly but the Standard Slope changes slowly. Therefore, no single parameter is a good measure of SNR change over a wide range of values. Thus, a joint metric based on Kurtosis and Standard Slope is proposed in the next section for TOA estimation.

Based on the results in Section 4.5, a joint metric for TOA estimation is formulated as

$$Sm = \frac{K - SS}{10} \tag{18}$$

Where K is the Kurtosis and SS is the Standard Slope.

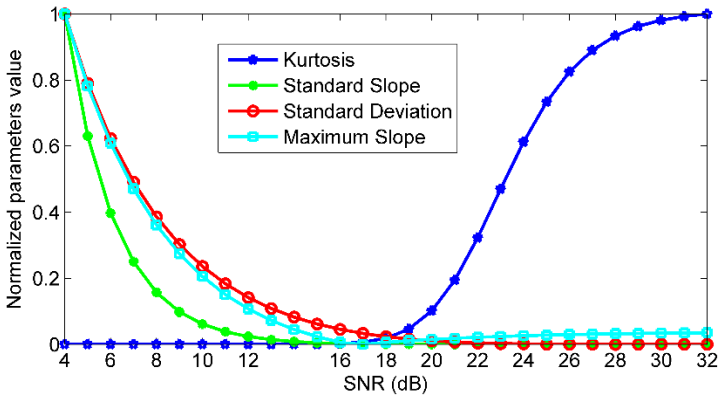

Figure 4. Four Parameters Change with SNR in CM1.1 with $T_i = 1ns$

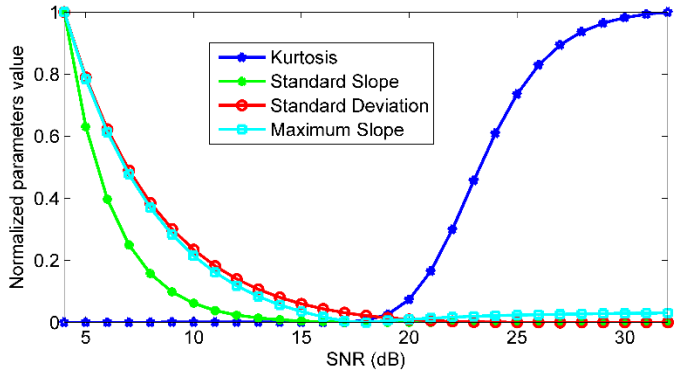

Figure 5. Four Parameters Change with SNR in CM1.1 with $T_i = 3ns$

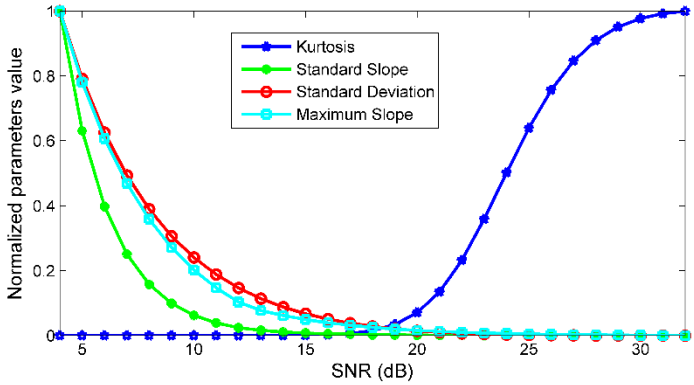

Figure 6. Four Parameters Change with SNR in CM 2.1 with $T_i = 1ns$

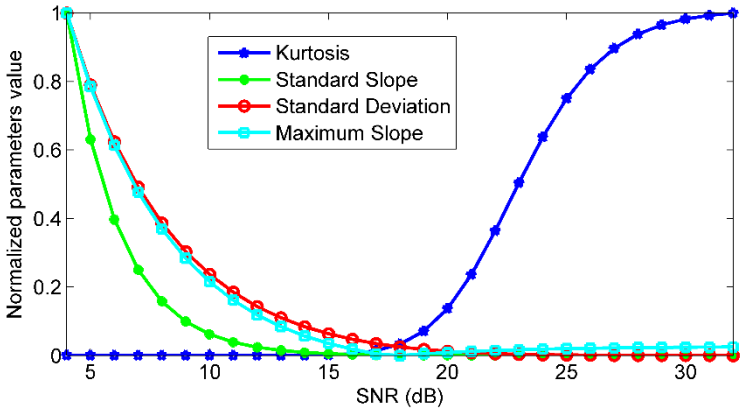

Figure 7. Four Parameters Change with SNR in CM 2.1 with $T_i = 3ns$

5. Threshold Based on Kurtosis and Standard Slope

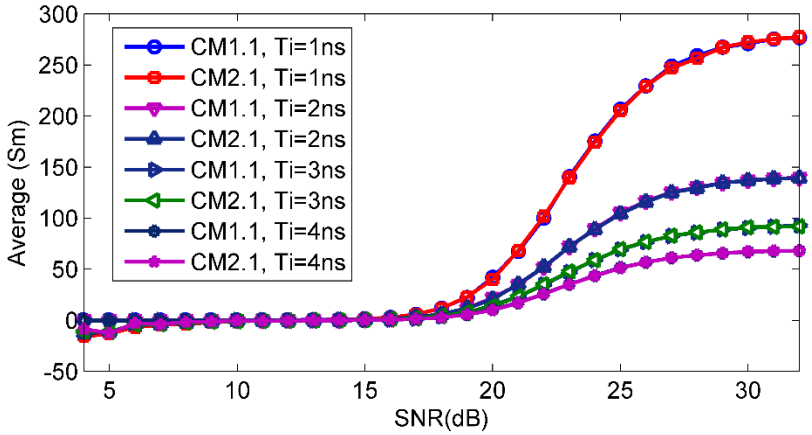

Figure 8. Average Values with Respect to SNR for Different CM and T_i

5.1. Relationship between Sm and SNR

In order to verify the relationship between the proposed metric Sm and SNR, 1000 channel realizations were generated when SNR is from 4dB to 32dB in each IEEE802.15.3c channel. The average values of Sm are presented in the Figure 8. The results show that Sm is a monotonic function for a large range of SNR values, and it is even much more sensitive to changes in SNR. The eight fixed curves differ somewhat due to the channel model and integration period used. The figure shows that Sm is more sensitive to T_i .

5.2. Relationship between MAE and the Normalized Threshold

In order to determine the best threshold (ξ_{best}) based on *Sm*, the relationship between MAE and normalized threshold (ξ_{norm}) was investigated. 1000 channel realizations with SNR={4, 5,…, 32}dB were simulated under CM1.1 and CM2.1 environments. ξ is the threshold which is compared to the energy values to find the first threshold crossing. When ξ is bigger than $z[n_{\max}]$, we can't get the TOA estimation, so in this case, ξ is set

to $z[n_{\max}]$. To illustrate the results, Figures 9 shows the relationship between MAE and the Normalized Threshold in the CM1.1 and CM2.1 channels, respectively, with T_i is1ns, 2ns and 3ns. The relationship is always that the MAE decreases as *Sm* increases. Another conclusion is that the minimum MAE is lower as J increases. The normalized threshold ξ_{norm} with respect to the minimum MAE is just the best threshold ξ_{best}. The relationship between ξ_{best} and Sm will be shown in the next section.

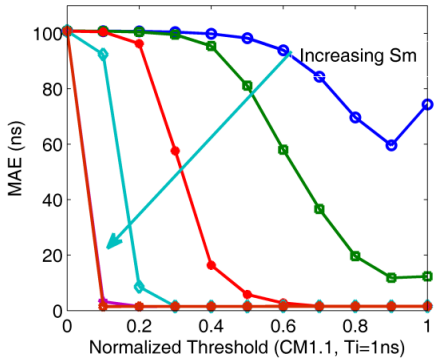

Figure 9.1. CM1.1 and $T_i = 1ns$

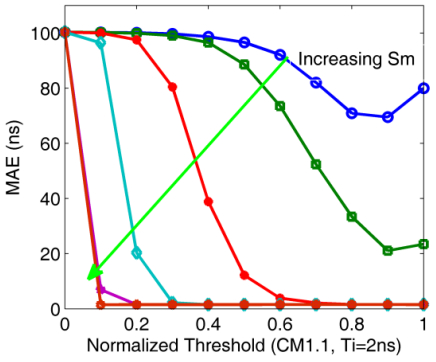

Figure 9.2. CM1.1 and $T_i = 2ns$

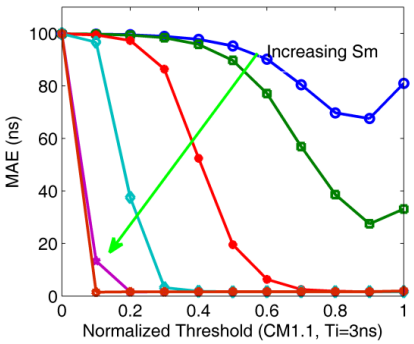

Figure 9.3. CM2.1 and $T_i = 3ns$

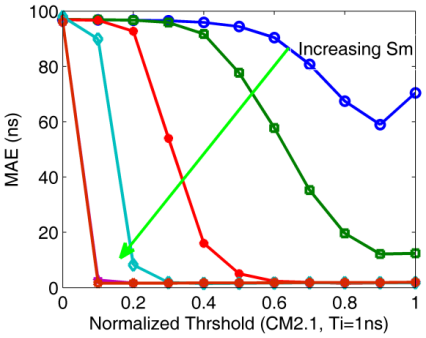

Figure 9.4. CM2.1 and $T_i = 1ns$

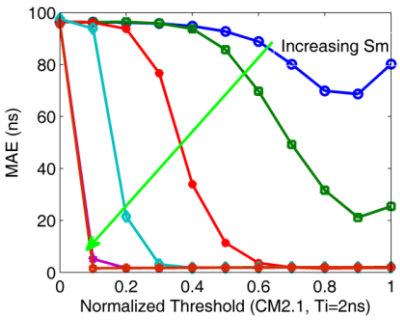

Figure9.5. CM2.1 and $T_i = 2ns$

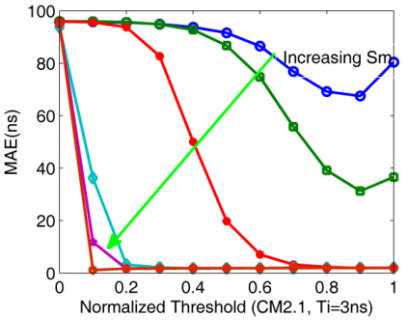

Figure9.6. CM2.1 and $T_i = 3ns$

Figure 9. MAE with Respect to Normalized Threshold

5.3. Normalized Threshold with Sm

From the results in the previous section, the relationship between ξ_{best} and Sm shows in Figure 10(1ns), Figure 11(2ns), Figure 12(3ns) and Figure 13(4ns) for each value of Sm. This shows that the relationship between the two parameters is not affected significantly by the CM, but is more dependent on the integration period. Therefore, four piecewise functions were fitted to these results aiming at $T_i = (1ns, 2ns, 3ns, 4ns)$. The relationship can be described as expression (19), expression (20), expression (21) and expression (22).

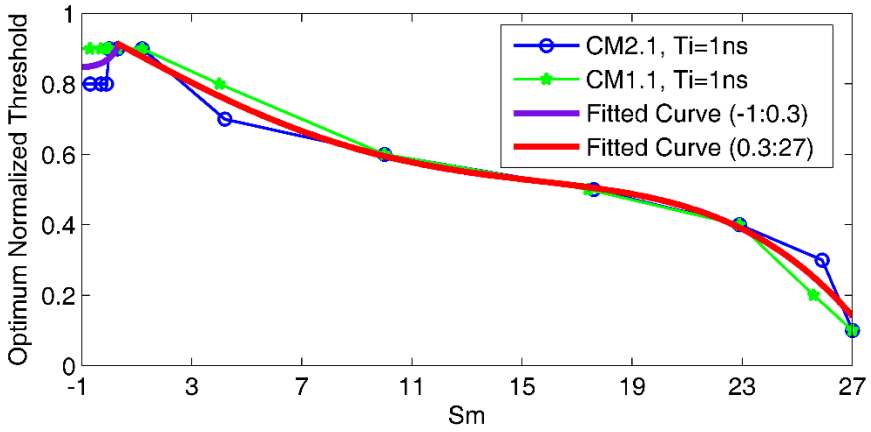

Figure 10. Normalized Threshold with Respect to Sm T_i =1ns

$$\xi_{best} = \begin{cases} 0.845 + 2.85e^{2.4248x-2} & -1.5 \le x < 0.3 \\ -4.509e^{-6}x^4 + 1.427e^{-4}x^3 - 8.276e^{-5}x^2 - 4.217e^{-2}x + 0.9273 & 0.3 \le x \end{cases} \quad (19)$$

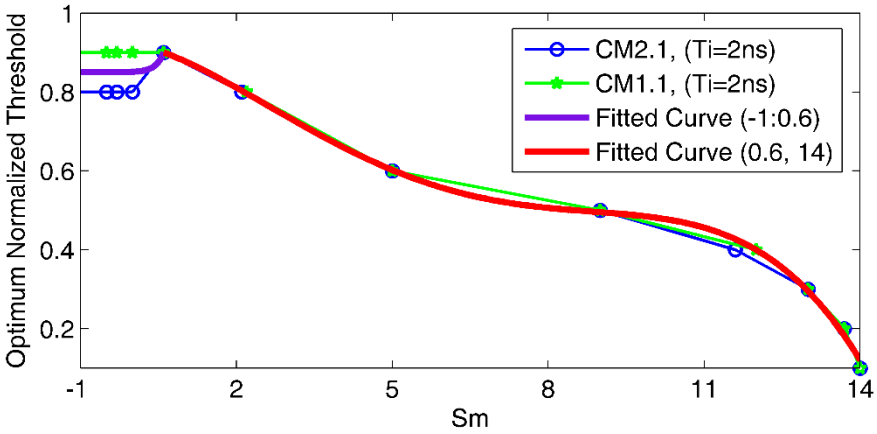

Figure 11. Normalized Threshold with Respect to Sm T_i =2ns

$$\xi_{best} = \begin{cases} 0.8499 + e^{6.5428x-3} & -1.3 \le x < 0.6 \\ -1.364e^{-4}x^4 + 3.135e^{-3}x^3 - 1.909e^{-2}x^2 - 3.041e^{-2}x + 0.9246 & 0.6 \le x \end{cases} \quad (20)$$

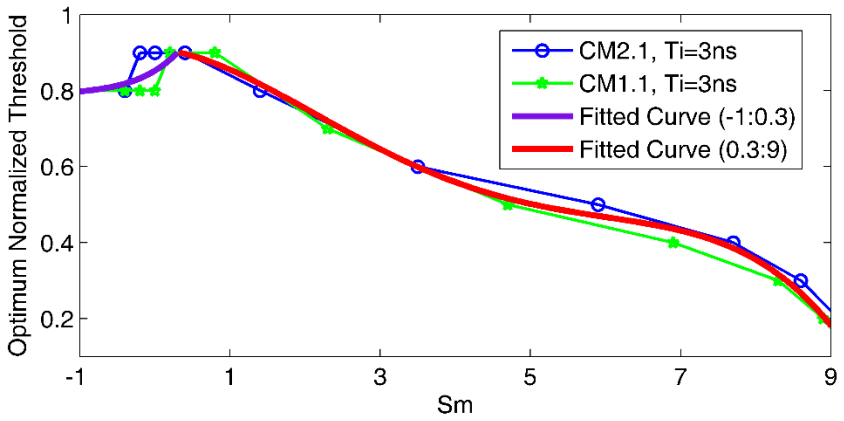

Figure 12. Normalized Threshold with Respect to Sm T_i =3ns

$$\xi_{best} = \begin{cases} 0.7877 + 6.47e^{1.8651x-2} & -1.1 \le x < 0.3 \\ -6.806e^{-4}x^4 + 1.107e^{-2}x^3 - 5.203e^{-2}x^2 - 1.312e^{-2}x + 0.9098 & 0.3 \le x \end{cases} \quad (21)$$

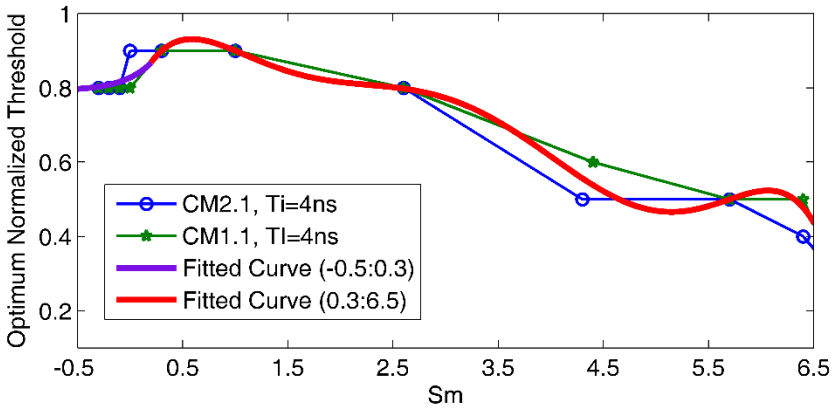

Figure 13. Normalized Threshold with Respect to Sm T_i =4ns

$$\xi_{best} = \begin{cases} 0.7913 + 3.62e^{3.7268x-2} & -1.1 \le x < 0.3 \\ -1.285e^{-3}x^6 + 2.515e^{-2}x^5 - 0.1856x^4 + 0.645x^3 - 1.086x^2 + & \\ 0.744x + 0.7585 & 0.3 \le x \end{cases} \quad (22)$$

6. Results and Discussion

In this section, the MAE is examined for different TOA estimation algorithms which based on Energy Detector in the IEEE 802.15.3c CM1.1 and CM2.1 channels. As before, 1000 channel realizations are generated for each case. A 2PPM-TH-60GHz signal is employed, and the received signal is sampled at $f_c = 1 \cdot e^{10}$ Hz. The other system parameters are $T_f = 200ns$, $T_c = 1ns$ the value of T_i is from 1ns to 4ns and *N*=1. Each realization has a TOA uniformly distributed within (0-T_f). The MAE for SNR values from 4dB to 32dB in LOS (CM1.1) is presented in the Figure 14 ($T_i = 1ns\ and\ 4ns$) and Figure 15 ($T_i = 1ns\ and\ 4ns$). At the same time, The MAE for SNR values from 4dB to 32dB in NLOS (CM2.1) is presented in the Figure 16($T_i = 1ns\ and\ 4ns$) and Figure

17($T_i = 2ns\ and\ 3ns$). This shows that the proposed algorithm performs even much better than other algorithm such as MES and FT. The performance in CM1.1 is better than in CM2.1 aiming at the same T_i when SNR<22dB, MAE for CM2.1 can get even much better results when SNR<22dB. In most cases, the performance with $T_i = 1ns$ is better than that with $T_i = 2ns, 3ns and\ 4ns$ regardless of the channel. Figures 14-17 present the MAE performance with three TOA algorithms in channels CM1.1 and CM2.1, respectively. Here "Joint Metric" refers to the proposed algorithm, "MES" is the Maximum Energy Selection algorithm, and the normalized threshold for the Fixed Threshold algorithm is set to 0.4. As expected based on the results in Section 5, the MAE with the proposed algorithm is lower than with other algorithms, particularly at low to moderate SNR values. The proposed algorithm is better except when the SNR is greater than 24dB. The performance of the proposed algorithm is more robust than the other algorithms, as the performance difference is very small compared to the difference with other algorithms. For almost all SNR values the proposed algorithm is even much better. Conversely, the performance of other algorithms varies greatly and is very bad for low to moderate SNR values.

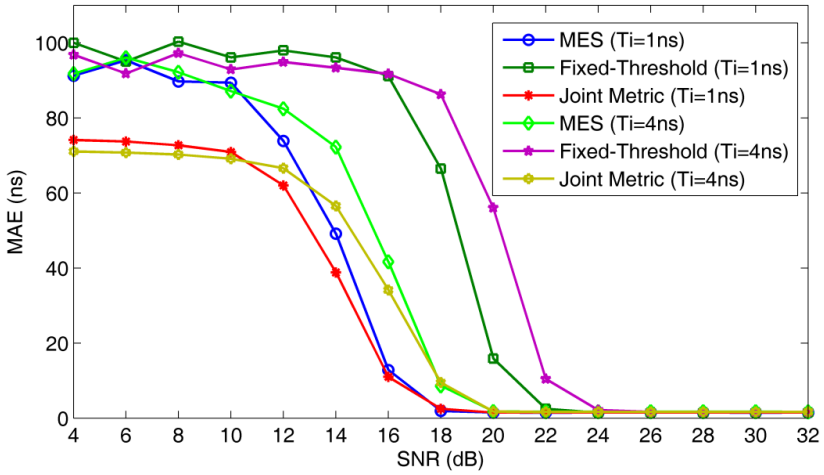

Figure 14. MAE for Different Algorithms with CM1.1 with T_i =1ns and 4ns

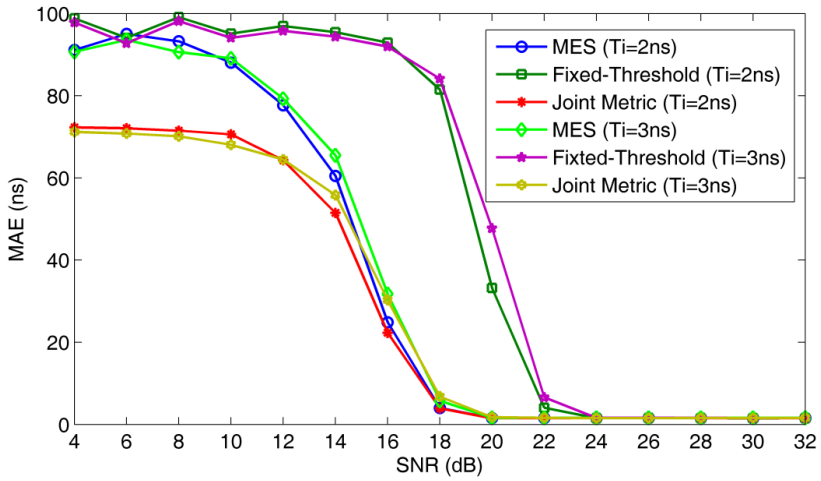

Figure 15. MAE for Different Algorithms with CM1.1 with T_i =2ns and 3ns

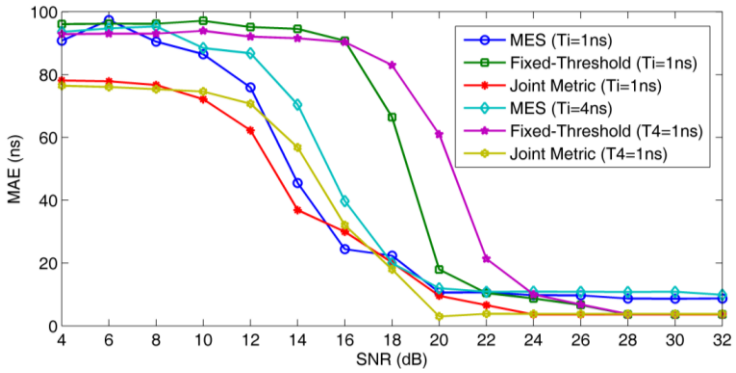

Figure 16. MAE for Different Algorithms with CM2.1 with T_i =1ns and 4ns

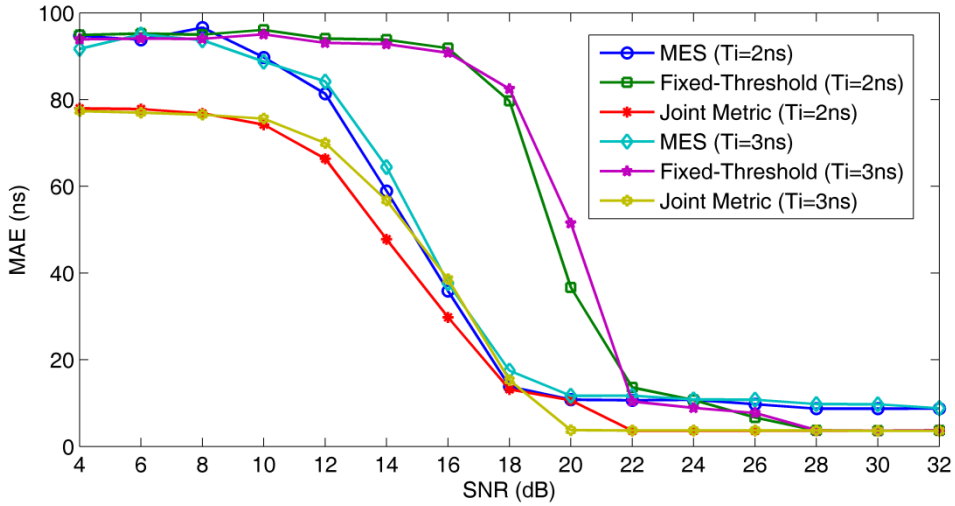

Figure 17. MAE for Different Algorithms with CM2.1 and T_i =2ns and 3ns

7. Conclusions

In this paper, a novel TOA estimation algorithm is proposed which is based on Energy Detector for 60GHz ranging, positioning and tracking applications. Here we study the relationships between SNR and four typical parameters such Kurtosis, Standard Deviation, Maximum Slope and Standard Slope, the results show that Kurtosis and Standard Slope can respect the SNR information bitterly. So we proposed a novel algorithm based on a new joint parameter using Kurtosis and Standard Slope. At the same time, the best normalized threshold was determined using simulation with the CM1.1 and CM2.1 channels and curve fitting. The effects of the integration period and channel model were investigated. It was determined that the proposed threshold selection technique is largely independent of the channel model. The performance of the proposed algorithm was shown to be better than several known algorithms. In addition, the proposed algorithm is more robust to changes in the SNR and integration period.

Acknowledgments

The authors would like to thank colleagues from the UWB Laboratory in the College of Information Science and Engineering, Ocean University of China, for help with obtaining the measurement data. This work was supported by the Nature Science Foundation of China under Grant No. 60902005, the Qingdao International Science and Technology Cooperation Projects of Qingdao under Grant No. 12-1-4-137-hz, and the

Qingdao Transformation of Scientific and Technological Achievements Guiding Plan (youth special program) under Grant No. 14-2-4-37-jch.

References

[1] L. Zhang, "A fully integrated 60GHz four channel CMOS receiver with 7GHz ultra-wide band width for IEEE 802.11ad standard", Communication, vol. 11, no. 6, **(2014)**, pp. 42-50, China.
[2] S.K. Yong and C.C. Chong, "An overview of multi gigabit wireless through millimeter Wave Strategy: Potentials and Technical Challenges", EURASIP J. Wireless Communications and Networking, vol. 2007, no. 1, **(2007)**, pp. 1-10.
[3] R.C. Daniels and R.W. Heath, "60 GHz wireless communications: emerging requirements and design recommendations", IEEE Vehicular Strategy Society, vol. 2, **(2007)**, pp. 41-50.
[4] C.C. Chong, F.M. Peter and Smulders, "60GHz-Millimeter-Wave Radio Principle, Strategy, and News Results", EURASIP Journal on Wireless Communications and Networking, vol. 2007, no. 1, **(2007)**, pp. 1-8.
[5] S.K. Yong, P.F. Xia and V.G. Alberto, "60-GHz Strategy for Gbps WLAN and WPAN: From Theory to Practice", **(2013)**, Beijing: Press of China Machine.
[6] R.C. Daniels and R.W. Health, "60 GHz wireless communications: emerging requirements and design recommendations", IEEE Vehicular Strategy Magazine, vol. 2, no. 3, **(2007)**, pp. 41-50.
[7] D. Jie, X. Cui, H. Zhang and G. Wang, "An ultra-wideband location algorithm based on neural network". International Conference on Wireless Communications Networking and Mobile Computing (WiCOM), vol. 11, no. 6, (**2010)**, pp. 56-64.
[8] X. Tu, H. Zhang, X. Cui and T.A. Gulliver, "3D TDOA/AOA location based on extended Kalman filter", International Symposium on Antennas, Propagation and EM Theory (ISAPE), vol. 11, no. 6, (**2010)**, pp. 56-64.
[9] Z. Sahinoglu and S. Gezici, "Ranging in the IEEE 802.15.4a standard", in IEEE Wireless and Microwave Strategy Conference (WAMICON), **(2006)**.
[10] D. Dardari, A. Conti, U. Ferner, A. Giorgetti and M.Z. Win, "Ranging with ultra-wide bandwidth signals in multipath environments", Proceedings of the IEEE, vol. 97, no. 2, (**2009)**, pp. 404-426.
[11] Y. Zhang, A.K. Brown, W.Q. Malik, and D.J. Edwards, "High resolution 3D angle of arrival determination for indoor UWB multipath propagation", IEEE Transactions on Wireless Communications, vol. 7, no. 8, (**2010)**, pp. 3047-3055.
[12] D. Dardari, A. Giorgetti and M.Z. Win, "Time of arrival estimation of UWB signals in the presence of narrowband and wideband interference", IEEE International Conference on Ultra-Wideband (ICUWB), **(2007)**.
[13] M. Bocquet, C. Loyez and A. BenlarbiDelai, "Using enhanced TDOA measurement for indoor localization", IEEE Microwave and Wireless Components Letters, vol. 15, no.10, **(2005)**, pp. 612-614.
[14] A. Abbasi and M.H. Kahaei, "Improving source localization in LOS and NLOS multipath environments for UWB signals", International CSI Computer Conference (CSICC), **(2009)**.
[15] I. Guvenc and Z. Sahinoglu, "Multi-scale energy products for TOA estimation in IRUWB systems", IEEE Global Telecommunications Conference, (GLOBECOM), **(2005)**.
[16] A.Y.Z. Xu, E.K.S. Au, A.K.S. Wong and Q. Wang, "A novel threshold based coherent TOA estimation for IR-UWB systems", IEEE Transactions on Vehicular Strategy, vol. 58, no. 8, **(2009)**, pp. 4675-4681.
[17] I. Guvenc and Z. Sahinoglu, "Threshold selection for UWB TOA estimation based on kurtosis analysis", IEEE Communications Letters, vol. 9, no. 12, **(2005)**, pp. 1025-1027.
[18] I. Guvenc and Z. Sahinoglu. "Threshold based TOA estimation for impulse radio UWB systems", IEEE International Conference on Ultra-Wideband, **(2005)**.
[19] "IEEE Standard for Information strategy--Local and metropolitan area networks--Specific requirements--Part 15.3, Wireless Medium Access Control (MAC) and Physical Layer (PHY) Specifications for High Rate Wireless Personal Area Networks (WPAN) amendment 2:millimeter-wave-based alternative physical layer extension", IEEE Computer Society, IEEE 802.15.06-0474-00-003c, **(2009)**, New York, USA.
[20] "802.11n-2009-IEEE Standard for Information strategy-- Local and metropolitan area networks--Specific requirements--Part 11, Wireless LAN Medium Access Control (MAC)and Physical Layer (PHY) Specifications Amendment 5, Enhancements for Higher Throughput", IEEE Computer Society, IEEE 978-0-7381-6731-2, **(2009)**, New York, USA.
[21] C.R. Andersonn and T.S. Rappaport, "In-building wideband partition loss measurements at 2.5 and 60GHz", IEEE Transactions on Wireless Communications, vol. 3, no. 3, **(2004)**, pp. 922-928.
[22] S. Collong, G. Zaharia and G.E. Zein, "Influence of the human activity on wide-band characteristics of the 60GHz indoor radio channel", IEEE Transactions on Wireless Communications, vol. 3, no. 6, **(2005)**, pp. 2396-2406.
[23] A. Maltsev, R. Maslennikov and A. Sevastyanov, "Experimental investigations of 60GHz WLAN systems in office environment", IEEE Journal on Selected Areas in Communications, vol. 27, no. 8, **(2009)**, pp. 1488-1499.

[24] M.G. Sanchez, A.V. Alejos and I. Cuinas, "Comparision of space deversity performance in indoor radio channels at 40GHz and 60GHz", Proc. of European Conference on Wireless Strategy, **(2008)**, Amsterdam**.**
[25] H.B. Yang, "Channel characteristics and transmission performance for various channel configurations at 60GHz", EURASIP Journal on Wireless Communications and Networking, vol. 2007, no. 1, **(2007)**, pp. 43-43.
[26] N. Li, "Study on the properties of 60 GHz impulse radio communication system", Qingdao, Ocean University of China, **(2012)**.
[27] X. Cui, C. Wu and J. Li, "UWB simulation of energy detection algorithm based on the Internet of things", Application of micro-computer, vol. 27, no. 9, **(2011)**, pp.20-26.

Authors

Xiao-Lin Liang, He now studies in College of Information Science and Engineering and is a master candidate in Ocean University of China. His research interests include ultra-wideband radio systems, 60GHz wireless communication system.

Ting-Ting Lu, She received the Ph. D. degree in College of Information Science and Engineering from Ocean University of China in 2013. She is now a lecture in College of Information Science and Engineering. Her research interests include ultra-wideband radio systems, 60GHz wireless communication system.

Hao Zhang, He received the MBA degree in New York Institute of Technology, American in 2001 and the Ph. D. degree in Electrical and Computer Engineering from the University of Victoria, Canada in 2004. He was a Project Manager for Microsoft Inc. in United States during January 2000-May 2000. During 2004-2008, he was the Vice President for the United States Gamma Capital Inc. He is now an Adjunct Assistant Professor in the Department of Electrical and Computer Engineering. Also he becomes a professor and the Ph. D. supervisor in College of Information Science and Engineering from Ocean University of China in 2006. His research concerns ultra-wideband radio systems, 60GHz wireless communication system and MIMO wireless communication.

T. Aaron. Gulliver received the Ph. D. degree in Electrical and Computer Engineering from the University of Victoria, Canada in 1989. He is now a professor and the Ph. D. supervisor in the Department of Electrical and Computer Engineering. In 2002, he becomes a Fellow of the Engineering Institute of Canada, and in 2012 a Fellow of the Canadian Academy of Engineering. He is also a senior member of IEEE. His research concerns information theory and communication theory, algebraic coding theory and smart grid and ultra wideband communication.

